23 Oct 2018

Multifidelity Modeling of Ultrasonic Testing Simulations with Cokriging

Leifur Leifsson

Xiaosong Du
Missouri University of Science and Technology, xdnwp@mst.edu

Slawomir Koziel

Recommended Citation

L. Leifsson et al., "Multifidelity Modeling of Ultrasonic Testing Simulations with Cokriging," *2018 IEEE MTT-S International Conference on Numerical Electromagnetic and Multiphysics Modeling and Optimization, NEMO 2018*, article no. 8503399, Institute of Electrical and Electronics Engineers, IEEE, Oct 2018.
The definitive version is available at https://doi.org/10.1109/NEMO.2018.8503399

Multifidelity Modeling of Ultrasonic Testing Simulations with Cokriging

Leifur Leifsson
Dep. of Aerospace Engineering
Iowa State University
Ames, IA 50011, USA
leifur@iastate.edu

Xiaosong Du
Dep. of Aerospace Engineering
Iowa State University
Ames, IA 50011, USA
xiaosong@iastate.edu

Slawomir Koziel
Eng. Opt. & Modeling Center
Reykjavik University
Reykjavik, Iceland
koziel@ru.is

***Abstract*—Multifidelity methods are introduced to the nondestructive evaluation (NDE) of measurement systems. In particular, Cokriging interpolation metamodels of physics-based ultrasonic testing (UT) simulation responses are utilized to accelerate the uncertainty propagation in model-assisted NDE. The proposed approach is applied to a benchmark test case of UT simulations and compared with the current state-of-the-art techniques. The results show that Cokriging captures the physics of the problem well and is able to reduce the computational burden by over one order of magnitude compared to the state of the art. To the best of the author's knowledge, this the first time multifidelity methods are applied to model-assisted NDE problems.**

Keywords—nondestructive evaluation; ultrasonic testing; simulations; metamodeling; polynomial chaos expansions; kriging; cokriging.

I. Introduction

Uncertainty propagation (UP) plays an important role in model-assisted nondestructive evaluation (NDE) [1]. In particular, UP is needed in model-assisted probability of detection (MAPOD), and defect characterization to quantify the influence of uncertain input parameters on nondestructive testing (NDT) systems [2, 3]. Examples of NDT systems include ultrasonic testing (UT) and eddy current testing.

Current state-of-the-art UP techniques used in NDE use Monte Carlo sampling (MCS) either on the true physics-based simulation model or on metamodel approximations of the physics-based simulations [4]. Recent development in modeling of NDT systems have realized accurate simulation models [5]. However, these models are time-consuming to evaluate, often on the order of six hours on a high-performance computing clusters. Moreover, the NDT systems under consideration typically have a large number uncertain input parameters, anywhere from a handful to tens or even hundreds. Clearly, MCS on the true model can then be impractical. In some cases, even the use of metamodels, such as Kriging interpolation [6], can be challenging.

In this work, multifidelity methods are introduced to NDE area for the first time, to the best of the author's knowledge, and applied to the uncertainty propagation of UT simulation models. Multifidelity methods are used to fuse information of varying degrees of fidelity. In particular, multifidelity methods leverage the speed of low-fidelity models to reduce the computational burden, while guaranteeing that the accuracy of the results are at the high-fidelity level. The work presented in this paper uses the fusion-based Cokriging metamodel [7] to construct a fast and accurate multifidelity model of high- and low-fidelity UT simulations.

The paper is organized as follows. The UT simulation models are described in Section II. Section III gives the details of the metamodeling methods. The proposed approach is applied to two-parameter test case and compared to state-of-the-art methods in Section IV. The paper ends with conclusion.

II. Ultrasonic Testing Simulations

In tfhis work, a benchmark UT problem is utilized to evaluate the proposed approach. The benchmark problem involves a spherically-void-defect in a fused quartz block. The ultrasonic testing is carried out in water using a spherically focused transducer of radius 6.23 mm and a frequency range of 0 Hz to 10MHz. Figure 1 shows the setup of the benchmark case.

The high-fidelity UT simulation is the Thompson-Gray model based on the paraxial approximation of the incident and scattered ultrasonic waves [8]. The model computes the spectrum of voltage at the receiving transducer in terms of the velocity diffraction coefficients of the transmitting/receiving transducers, scattering amplitude of the defect and a frequency-dependent coefficient known as the system-efficiency function. Here, the velocity diffraction coefficients are calculated using the multi-Gaussian beam model, and the scattering amplitude of the spherical-void is calculated using the method of separation of variables. The system efficiency function, which is a function of the properties and settings of the transducers and the pulser was taken from the WFNDEC archives. The time-domain pulse-echo waveforms are computed by performing fast Fourier transform on the voltage spectrum.

The low-fidelity UT simulation model is based on the same model as the high-fidelity one but with a simplified physics model. In particular, the low-fidelity model uses the Kirchhoff approximation to calculate the scattering [9]. This simplifies the computation and speeds it up. However, the resulting model is not as accurate

To validate the models on the benchmark problem mentioned above, they are compared against experimental data, shown in Fig. 2. The high-fidelity model (denoted as SOV) matches well with the experimental data, whereas the low-fidelity one (denoted by KA) captures the overall trend well but is not as accurate.

978-1-5386-5204-6/18/$31.00 ©2018 IEEE

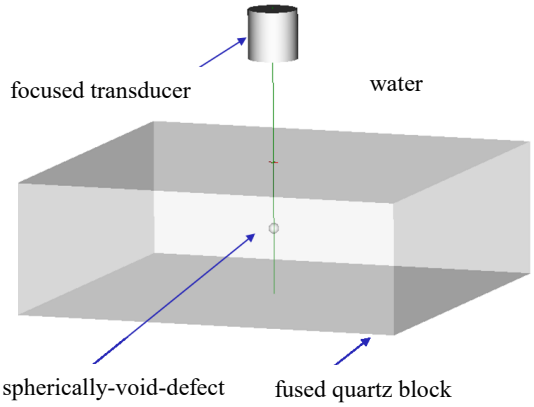

Fig. 1. Setup of the spherically-void defect benchmark test case.

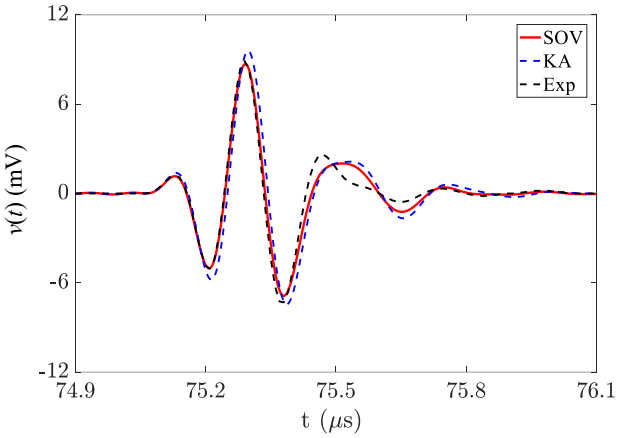

Fig. 2. Comparison of the amplitude responses of the UT simulation models with expermental measurements of a defect of 0.34 mm diameter. Here, SOV is the high-fidelity model response and KA is the low-fidelity one.

III. Metamodeling

This section starts by describing two of the current state-of-the-art metamodeling techniques used for UT simulations, PCE with ordinary least squares (OLS) regression and Kriging, before describing the proposed multifidelity approach.

A. Polynomial Chaos Expansions

Polynomial chaos expansion (PCE) metamodels have the generalized formulation [10]

$$Y = M(\mathbf{X}) = \sum_{i=1}^{\infty} \alpha_i \mathbf{\Psi}_i(\mathbf{X}), \tag{1}$$

where $\mathbf{X} \in \mathbb{R}^m$ is a vector with random independent components described by a probability density function f_X, $Y \equiv M(\mathbf{X})$ is a map of $\mathbf{X}$, i is the index of ith polynomial term, $\mathbf{\Psi}$ is multivariate polynomial basis, and α is corresponding coefficient of basis function. In practice, a truncated form of the PCE is used

$$M(\mathbf{X}) \approx M^{PC}(\mathbf{X}) = \sum_{i=1}^{P} \alpha_i \mathbf{\Psi}_i(\mathbf{X}), \tag{2}$$

where $M^{PC}(\mathbf{X})$ is the approximate truncated PCE model, and P is the total number of sample points and can be calculated as

$$P = \frac{(p+n)!}{p!n!}, \tag{3}$$

where p is the order of the PCE, and n is the total number of random input variables.

Solving for the coefficients $\boldsymbol{\alpha}$ is formulated as a least-squares minimization problem

$$\hat{\boldsymbol{\alpha}} = \arg\min E[\boldsymbol{\alpha}^T \Psi(\mathbf{X}) - M(\mathbf{X})]. \tag{4}$$

In this work, the ordinary least-squares (OLS) method is used to solve (4) using

$$\hat{\boldsymbol{\alpha}} = (\mathbf{A}^T\mathbf{A})^{-1}\mathbf{A}^T\mathbf{Y}, \tag{5}$$

where $\mathbf{Y}$ is the vector of model responses, and $A_{ji} = \Psi_i(\mathrm{x}^j)$, $j = 1, \ldots, n$, $i = 1, \ldots, P$.

B. Kriging

Given the training set $\mathbf{X}_{B.KR} = \{\mathbf{x}_{KR}{}^1, \mathbf{x}_{KR}{}^2, \ldots, \mathbf{x}_{KR}{}^{NKR}\} \subset \mathbf{X}_R$ be the base (training) set and $\mathbf{s}(\mathbf{X}_{B.KR})$ the corresponding surrogate model responses. The kriging interpolant is derived as [11]

$$\mathbf{s}_{KR}(\mathbf{x}) = \mathbf{M}\boldsymbol{\alpha} + \mathbf{r}(\mathbf{x}) \cdot \mathbf{\Psi}^{-1} \cdot (\mathbf{s}(\mathbf{X}_{B.KR}) - \mathbf{F}\boldsymbol{\alpha}), \tag{6}$$

where $\mathbf{M}$ and $\mathbf{F}$ are Vandermonde matrices of the test point $\mathbf{x}$ and the base set $\mathbf{X}_{B.KR}$, respectively. The coefficient vector $\boldsymbol{\alpha}$ is determined by generalized least squares. $\mathbf{r}(\mathbf{x})$ is an $1 \times N_{KR}$ vector of correlations between the point $\mathbf{x}$ and the base set $\mathbf{X}_{B.KR}$, where the entries are $r_i(\mathbf{x}) = \mathbf{\Psi}(\mathbf{x}, \mathbf{x}_{KR}{}^i)$, and $\mathbf{\Psi}$ is a $N_{KR} \times N_{KR}$ correlation matrix, with the entries given by $\Psi_{i,j} = \mathbf{\Psi}(\mathbf{x}_{KR}{}^i, \mathbf{x}_{KR}{}^j)$. In this work, the exponential correlation function is used, i.e., $\mathbf{\Psi}(\mathbf{x}, \mathbf{x}') = \exp(\sum_{k=1,\ldots,n} -\theta_k |x_k - x'_k|)$, where the parameters $\theta_1, \ldots, \theta_n$ are identified by maximum likelihood estimation (MLE). The regression function is chosen as $\mathbf{F} = [1 \ldots 1]^T$ and $\mathbf{M} = (1)$.

C. Cokriging

The generation of the cokriging model is carried out through a sequential construction of two kriging models: the first model $\mathbf{s}_{KR}$ composed from the physics-based metamodel training samples ($\mathbf{X}_{B.KR}$, $\mathbf{s}_{KR}(\mathbf{X}_{B.KR})$), and the second $\mathbf{s}_{KRd}$ model generated on the residuals of the high- and low-fidelity samples ($\mathbf{X}_{B.KRf}$, $\mathbf{s}_d$), where $\mathbf{s}_d = \mathbf{f}(\mathbf{X}_{B.KRf}) - \rho \cdot \mathbf{s}_{KR}(\mathbf{X}_{B.KRf})$. The parameter ρ is a part of MLE of the second model.

The cokriging model $\mathbf{s}_{CO}(\mathbf{x})$ is defined as [12]

$$\mathbf{s}_{CO}(\mathbf{x}) = \mathbf{M}\boldsymbol{\alpha} + \mathbf{r}(\mathbf{x}) \cdot \mathbf{\Psi}^{-1} \cdot (\mathbf{s}_d - \mathbf{F}_{CO}\boldsymbol{\alpha}), \tag{7}$$

where the block matrices $\mathbf{M}$, $\mathbf{F}$, $\mathbf{r}(\mathbf{x})$ and $\mathbf{\Psi}$ can be written as a function of the two underlying Kriging models $\mathbf{s}_{KR}$ and $\mathbf{s}_{KRd}$:

$$\mathbf{r}(\mathbf{x}) = [\rho \cdot \boldsymbol{\sigma}^2 \cdot \mathbf{r}(\mathbf{x}), \rho^2 \cdot \boldsymbol{\sigma}^2 \cdot \mathbf{r}(\mathbf{x}, \mathbf{X}_{B.KR_f}) + \boldsymbol{\sigma}_d^2 \cdot \mathbf{r}_d(\mathbf{x})],$$

$$\mathbf{F}_{CO} = \begin{bmatrix} \mathbf{F} & 0 \\ \rho \cdot \mathbf{F}_d & \mathbf{F}_d \end{bmatrix}, \quad M = [\rho \cdot M_c \quad M_d],$$

and

$$\boldsymbol{\Psi} = \begin{bmatrix} \boldsymbol{\sigma}^2\boldsymbol{\Psi} & \rho \cdot \boldsymbol{\sigma}^2 \cdot \boldsymbol{\Psi}(\mathbf{X}_{B.KR}, \mathbf{X}_{B.KR_f}) \\ 0 & \rho^2 \cdot \boldsymbol{\sigma}^2 \cdot \boldsymbol{\Psi}(\mathbf{X}_{B.KR_f}, \mathbf{X}_{B.KR_f}) + \boldsymbol{\sigma}_d^2 \cdot \boldsymbol{\Psi}_d \end{bmatrix},$$

where ($\mathbf{F}$, $\boldsymbol{\sigma}$, $\boldsymbol{\Psi}$, $\mathbf{M}$) and ($\mathbf{F}_d$, $\boldsymbol{\sigma}_d$, $\boldsymbol{\Psi}_d$, $\mathbf{M}_d$) are matrices obtained from the $\mathbf{s}_{KR}$ and $\mathbf{s}_{KRd}$, respectively. Generally, $\boldsymbol{\sigma}^2$ and $\boldsymbol{\sigma}_d^2$ are process variances, while $\boldsymbol{\Psi}(\cdot,\cdot)$ and $\boldsymbol{\Psi}_d(\cdot,\cdot)$ stand for correlation matrices of two datasets with the optimized θ_k parameters and correlation function of $\mathbf{s}_{KR}$ and $\mathbf{s}_{KRd}$, respectively.

IV. Numerical Example

A. Problem Setup

The proposed approach is illustrated on the spherically-void-defect benchmark problem (Fig. 1) with two uncertain input parameters, the probe angle, θ, and the probe F-number, F, which are distributed as $N(0, 1)$ deg. and $U(13, 15)$, respectively. The objective is to model the peak amplitude of the UT simulation response as a function of the uncertain input parameters, and perform the uncertainty propagation.

The PCE metamodel with OLS and the Kriging metamodels are constructed using the high-fidelity model, whereas the Cokriging uses both the high- and the low-fidelity models. The metamodel construction is performed for defect sizes of 0.1 to 0.5 mm in increments of 0.1 mm. Latin hypercube sampling is used as the sampling scheme.

B. Results

Figure 3 shows the root mean squared error (RMSE), in mV, as a function of the number of samples of the high-fidelity model for a defect size of 0.5 mm. It can be seen that the Cokriging metamodel requires over one order of magnitude fewer high-fidelity samples than the current state-of-the-art metamodeling technique, Kriging in this case, to reach the desired accuracy level. The Cokriging model was setup using 1,000 low-fidelity model samples, which was determined by a parametric study. Figure 4 shows the variation of the normalized RMSE (NRMSE) with the defect size, indicating that the Cokriging metamodel is capable of reaching the same level of accuracy as the other two techniques across the defect size range.

Figures 5 and 6 show the convergence of the statistical moments in the uncertainty propagation for a defect size of 0.5 mm. The results show that the PCE metamodeling approach converges quickly towards the mean and the standard deviation. Note that the convergence of the PCE metamodel is achieved with using MCS. MCS using the Cokriging metamodel needs a large number of samples to converge. However, the Cokriging metamodel is fast to evaluate and the cost of the MCS is negligible compared to the cost of setting up the model. Moreover, MCS with the Cokriging metamodel is very similar to the MCS on the true model, which indicates that the Cokriging model captures well the output space of the true model. MCS with the Kriging metamodel requires significantly more samples to reach a converged result.

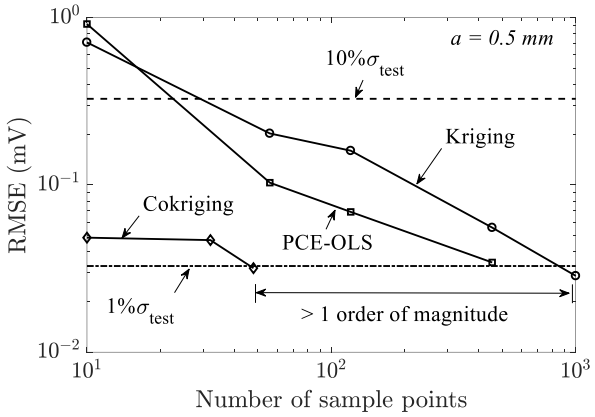

Fig. 3. Metamodeling setup cost for a defect size of 0.5 mm.

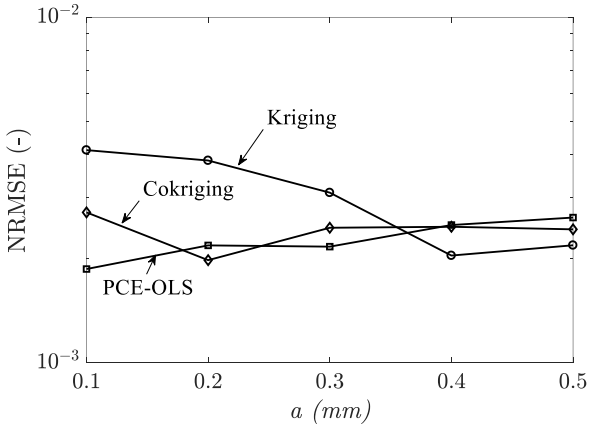

Fig. 4. Normalized error of the metamodels for different defect sizes.

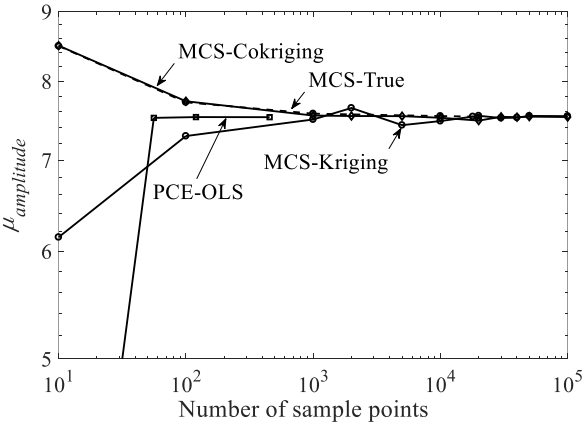

Fig. 5. Convergence on the mean for uncertainty propagation.

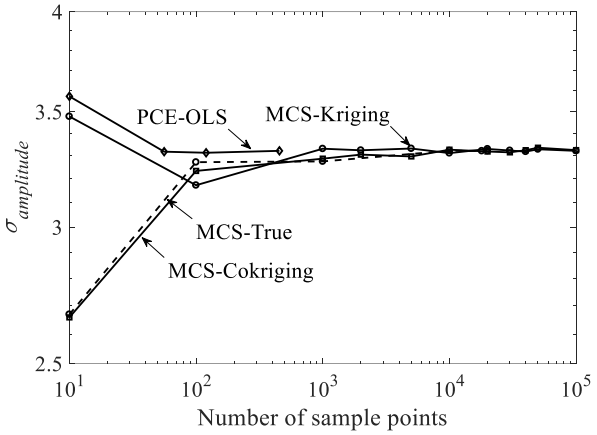

Fig. 6. Convergence on the standard deviation for uncertainty propagation.

V. Conclusion

Multifidelity modeling of ultrasonic testing simulations has been proposed in the context of model-assisted nondestructive evaluation (NDE). In particular, the multifidelity models were constructed using cokriging interpolation to accelerate the uncertainty propagation in the NDE process. The results show that the multifidelity method is promising for significantly reducing the computational burden of model-assisted NDE. Future work will consider NDE problems of higher complexity in terms of simulation model fidelity and parameter space dimensionality to further characterize the proposed approach.

Acknowledgment

This research was funded in part by the Center for Nondestructive Evaluation Industry/University Cooperative Research Program at Iowa State University (ISU), Ames, USA. The authors gratefully acknowledge Prof. Jiming Song at ISU for providing us with the ultrasonic testing simulation models and the experimental data for the model validation.

References

[1] J. Blitz, G. Simpson, "Ultrasonic Methods of Non-destructive Testing," London Chapman & Hall, 1996.

[2] B. Thompson, L. Brasche, D. Forsyth, E. Lindgren, and P. Swindell, "Recent Advances in Model-Assisted Probability of Detection," 4th European-American Workshop on Reliability of NDE, Berlin, Germany, June 2009.

[3] J. Aldrin, J. Knopp, E. Lindgren, and K. Jata, "Model-Assisted Probabiity of Detection Evaluation for Eddy Currnt Inspection of Fastener Sites," Review of Quantitative Nondestructive Evaluation, Vol. 28, 2009, pp. 1784-1791.

[4] M Darmon, S. Chatillon, S. Mahaut, P. Calmon, L. Fradkin, and V. Zernov, "Recent Advances in Semi-Analytical Scattering Models for NDT Simulation," Journal of Physics, Vol. 269, No. 1, 2011

[5] P Gurrala, K. Chen, J. Song, and R. Roberts, "Full Wave Modeling of Ultrasonic NDE Benchmark Problems Using Nystrom Method," 43rd Annual Review of Progress in Quantitative Nondestructive Evaluation, Vol. 36, 2017, pp. 150003-1 – 15000308.

[6] X. Du, R. Grandin, and L. Leifsson, "Surrogate Modeling of Ultrasonic Simulations Using Data-Driven Methods," 43rd Annual Review of Progress in Quantitative Nondestructive Evaluation, Vol. 36, 2016, pp. 150002-1 – 150002-9.

[7] S. Koziel, L. Leifsson, "Surrogate-Based Modeling and Optimization: Application in Engineering," Springer, 2010.

[8] T. Gray, "Ultrasonic Measurement Models – A Tribute to R Bruce Thompson," Reiview of Progress in Quantitative Nondestructive Evaluation, Vol. 31, No. 1, 2012, pp. 38-53.

[9] R. Grandin, T. Gray, R. Roberts, "Simulating UT Measurements from Bolthole Cracks," 42nd Annual Review of Progress in Quantitative Nondestructive Evaluation, Vol. 1706, 2016.

[10] G. Blatman, "Adaptive Sparse Polynomial Chaos Expansions for Uncertainty Propagation and Sensitivity Analysis," Ph.D. Thesis, Blaise Pascal University, 2009.

[11] J. Sacks, W. Welch, T. Michell, and H. Wynn, "Design and Analysis of Computer Experiments," Statistical Science, Vol. 4, 1989, pp. 409-423.

[12] H. Wackernagel, "Multivariate Geostatistics: An Introduction with Applications," Berlin, Germany: Spring-Verlag, 1995.